THE JOURNAL OF BIOLOGICAL CHEMISTRY
Vol. 279, No. 31, Issue of July 30, pp. 32667–32673, 2004

Printed in U.S.A.

Glutathione Limits Ero1-dependent Oxidation in the Endoplasmic Reticulum*

Received for publication, May 5, 2004
Published, JBC Papers in Press, May 25, 2004, DOI 10.1074/jbc.M404992200

Silvia Nerini Molteni‡, Anna Fassio‡§, Maria Rosa Ciriolo¶, Giuseppe Filomeni¶, Elena Pasqualetto‡, Claudio Fagioli‡, and Roberto Sitia‡‖**

From the ‡Department of Biological and Technological Research, San Raffaele Scientific Institute, 20132 Milano, Italy, ¶Dipartimento di Biologia, Università di Roma "Tor Vergata," 00133 Roma, Italy, and ‖Università Vita-Salute San Raffaele, 20132 Milano, Italy

Many proteins of the secretory pathway contain disulfide bonds that are essential for structure and function. In the endoplasmic reticulum (ER), Ero1α and Ero1β oxidize protein disulfide isomerase (PDI), which in turn transfers oxidative equivalents to newly synthesized cargo proteins. However, oxidation must be limited, as some reduced PDI is necessary for disulfide isomerization and ER-associated degradation. Here we show that in semipermeable cells, PDI is more oxidized, disulfide bonds are formed faster, and high molecular mass covalent protein aggregates accumulate in the absence of cytosol. Addition of reduced glutathione (GSH) reduces PDI and restores normal disulfide formation rates. A higher GSH concentration is needed to balance oxidative folding in semipermeable cells overexpressing Ero1α, indicating that cytosolic GSH and lumenal Ero1α play antagonistic roles in controlling the ER redox. Moreover, the overexpression of Ero1α significantly increases the GSH content in HeLa cells. Our data demonstrate tight connections between ER and cytosol to guarantee redox exchange across compartments: a reducing cytosol is important to ensure disulfide isomerization in secretory proteins.

The cytosol and the endoplasmic reticulum (ER)[1] are the main folding compartments of eukaryotic cells (1–3). The latter is the site of the production of proteins destined to the organelles of the central vacuolar system and to extracellular space. These molecules, collectively termed "secretory" proteins hereafter, are co-translationally translocated into the ER (4). Secretory proteins are designed to work in the extracellular environment, which differs substantially from the cytosol. Indeed their folding takes place in the ER, where the calcium concentration and the ratio between reduced glutathione (GSH) and oxidized glutathione (GSSG) resembles those that will be encountered in the extracellular environment. In the ER, secretory proteins undergo sequential processing steps, some of which are unique to this compartment (*i.e.* disulfide bond formation and *N*-linked glycosylation). These modifications are coupled to a tight quality control schedule that restricts transport to the Golgi apparatus to native conformers. Incompletely folded or assembled molecules are retained in the ER and eventually dislocated to the cytosol for proteasomal degradation (for reviews, see Refs. 1 and 5). In this respect, the ER can be viewed as a specialized and highly selective school wherein proteins are trained to acquire their functional native conformation.

A fundamental difference between cytosolic and secretory proteins is the abundance of disulfide bonds in the latter (6). Disulfides are often essential for folding and confer stability to secreted proteins (7). The abundance of ER resident oxidoreductases of the protein disulfide isomerase (PDI) family underscores their importance in the ER protein factory (6, 8). Disulfide bond formation requires that oxidizing conditions be maintained in this organelle. GSSG has long been considered the main source of oxidizing equivalents for the secretory pathway (9). However, yeast mutants deficient in glutathione synthesis can form disulfide bonds (10). Moreover, defects in Ero1p, the specific PDI oxidase, can be rescued by deletion of the *GSH1* gene, suggesting that in yeast, GSH competes with newly synthesized proteins for the oxidizing equivalents provided by Ero1p (11). Higher eukaryotes have two Ero1-like genes, Ero1α and Ero1β (12, 13). Both can oxidize PDI and promote disulfide formation (14).

The notion that expression of Ero1β is induced by ER stress provides a mechanism whereby cells can adjust the oxidative power of the ER when their protein load becomes excessive. However, cells face an equally important problem, that is preventing excessive oxidation within the ER. Indeed, disulfides must be isomerized during folding (15) and reduced prior to dislocation of terminally misfolded molecules targeted to proteasomal degradation (16). Inefficient degradation can lead to the accumulation of misfolded proteins in the ER and cytotoxicity (for review, see Ref. 17), thus underscoring the importance of precisely regulating the ER redox state.

In this study, we investigated the role of cytosolic factors, glutathione in particular, in controlling oxidative folding in higher eukaryotes, where this abundant tripeptide plays an important role also in regulating apoptosis (reviewed in Ref. 18). Moreover, we studied whether and how cells can sense and respond to the hyper-oxidation in the ER induced by Ero1α over-expression.

Our results demonstrate that GSH acts as the main antagonist of Ero1α, limiting disulfide bond formation in the ER.

* This work was supported in part by the Associazione Italiana per la Ricerca sul Cancro, Ministero della Sanita', Italian Ministry of University and Research (COFIN and Center of Excellence in Physiopathology of Cell Differentiation), and Telethon. The costs of publication of this article were defrayed in part by the payment of page charges. This article must therefore be hereby marked "*advertisement*" in accordance with 18 U.S.C. Section 1734 solely to indicate this fact.

§ Present address: Dipartimento di Medicina Sperimentale, Università di Genova, 16132 Genova, Italy.

** To whom correspondence should be addressed: Università Vita-Salute San Raffaele, Via Olgettina 58, 20132 Milano, Italy. Tel.: 39-02-2643-4722; Fax: 39-02-2643-4723; E-mail: r.sitia@hsr.it.

[1] The abbreviations used are: ER, endoplasmic reticulum; GSH, reduced glutathione; GSSG, oxidized glutathione; PDI, protein disulfide isomerase; DMEM, Dulbecco's modified Eagle's medium; JcM, Myc-tagged immunoglobulin J chain; BSO, DL-buthionine-[S,R] sulfoximine; DEM, diethyl maleate; DTT, dithiothreitol; NEM, *N*-ethyl maleimide; mPEG, monomethoxypolyethylene glycol; SP, semipermeable.

Interestingly, overexpressing Ero1α, but not an inactive mutant, induces a significant increase in the intracellular content of reduced glutathione, indicating the existence of intercompartmental compensatory pathways that maintain proper redox homeostasis.

EXPERIMENTAL PROCEDURES

Cells, Plasmids, and Reagents—HeLa cells were obtained from American Type Culture Collection and maintained in high-glucose Dulbecco's modified Eagle's medium (DMEM) supplemented with 5% fetal bovine serum and 1% penicillin/streptomycin.

Rabbit anti-PDI and rabbit anti-ribophorin antibodies were kind gifts of Drs. A. Benham and I. Braakman (Utrecht University, The Netherlands) and Dr. E. Ivessa (Vienna University, Austria), respectively. Anti-thioredoxin antibodies were produced by immunizing rabbits with purified human thioredoxin expressed in BL-21 *Escherichia coli* strain. The rabbit serum was subsequently analyzed for specificity. Only one band of the expected molecular mass (14.5 kDa) was identified by Western blotting with anti-thioredoxin.

Vectors for the expression of cytosolic red fluorescent protein (pDsRed2-N1) and ER-localized yellow fluorescent protein were purchased from Clontech. Myc-tagged immunoglobulin J chain (JcM), wild-type Ero1α, and the C394A-mutant are based on pcDNA3.1 expression vector (Invitrogen, San Giuliano Milanese, Italy) and have been described elsewhere (12, 14). The vector for the expression of a mutant ribophorin (Ri332) was generously provided by Dr. E. Ivessa (University of Vienna, Austria). 5000 monomethoxypolyethylene glycol (mPEG)-maleimide was purchased from Nektar Therapeutics, San Carlos, CA. All other chemicals were purchased from Sigma.

Transfections and Fluorescent Protein Detection—1.5×10^6 exponentially growing HeLa cells were plated on 100-mm dishes. The day after plating, cells were transfected with Lipofectin (Invitrogen) after the manufacturer's instructions. Twelve micrograms of expression vector were used for each cell culture dish.

For immunofluorescence analyses, HeLa cells were grown on glass coverslips, transfected to express yellow and red fluorescent proteins, and permeabilized as described below. Fluorescent images were taken by a fluorescence microscope equipped with a Hamamatsu charge-coupled device digital camera (Hamamatsu Photonics Italia, Arese, Italy).

Cell Permeabilization—For each sample, 6×10^6 HeLa cells transfected as above were harvested with Dulbecco's modified phosphate buffered saline (DPBS) containing 0.5 mM EDTA, washed with KHM buffer (110 mM potassium acetate, 2 mM magnesium acetate, 20 mM HEPES, pH 7.2) and permeabilized with 40 μg/ml digitonin in KHM buffer as described in Ref. 19. Then cells were washed once with HEPES buffer (50 mM potassium acetate, 90 mM HEPES, pH 7.2) and once with KHM buffer. After centrifugation, cells were resuspended in DMEM and used for the JcM oxidation assay.

GSH Deprivation—To decrease the cellular content of GSH, cells were treated overnight with 5 mM DL-buthionine-[S,R] sulfoximine (BSO), an inhibitor of γ-glutamyl cysteine synthetase. This treatment decreased GSH to about 20% of the initial amount. After BSO treatment, 2 mM diethyl maleate (DEM) was added to the culture medium, and cells were incubated for 1 h at 37 °C, just before the re-oxidation experiments.

JcM Oxidation Assay—The assay was performed as a modification of that described previously in Ref. 14. Briefly, JcM-transfected cells were resuspended in DMEM plus 5 mM dithiothreitol (DTT) and kept at 37 °C for 5 min to achieve disulfide bond reduction. After two washing steps at 4 °C to eliminate DTT, oxidation was obtained by incubating cells at 24 °C. After 0, 1, 2, 4, and 8 min, oxidation was stopped by the addition of *N*-ethyl maleimide (NEM) to each sample (final concentration 11 mM). Cells were then lysed in Nonidet P-40 lysis buffer (1% Nonidet P-40, 10 mM Tris, 150 mM NaCl, 20 mM NEM, protease inhibitors) and processed in a standard non-reducing SDS-PAGE, Western blot procedure.

PDI Redox State: Non-denaturing Gels—Intact or SP HeLa cells were incubated in DMEM with or without 10 mM DTT or 5 mM diamide for 10 min at 37 °C, washed twice in ice-cold DPBS containing 20 mM NEM, lysed in 50 mM Tris-Cl, pH 7.4, 150 mM NaCl, 1% Triton X-100, and analyzed by electrophoresis. Non-denaturing polyacrylamide gels were used to separate different redox forms of PDI. The following concentrations and pH were used. Resolving gel, 7.5% 29:1 acrylamide:bisacrylamide, 375 mM Tris-Cl, pH 8.8; stacking gel, 3% 29:1 acrylamide: bisacrylamide, 250 mM Tris-Cl, pH 6.8; running buffer, 5 mM Tris-Cl, pH 8, 38 mM glycine. Electrophoretic separation was performed at 4 °C, 10 mA per gel.

Thiol-alkylation Assay—HeLa cells were treated as described for non-denaturing gels, using 50 mM DTT or 10 mM diamide for 15 min at 37 °C. After two washes with cold PBS/10 mM NEM, cells were lysed in radioimmune precipitation assay buffer (150 mM NaCl, 50 mM Tris-Cl, pH 8, 0.1% SDS, 1% Nonidet P-40) containing 10 mM NEM and protease inhibitors. In these conditions, all accessible thiol-cysteines should be bound to NEM. Lysates were then incubated for 15 min at 50 °C with 50 mM DTT to obtain reduction of disulfides and then precipitated with 10% trichloroacetic acid. The trichloroacetic acid-insoluble material was resuspended in alkylating buffer (80 mM Tris-Cl, pH 6.8, 2% SDS, 25 mM 5000 mPEG-maleimide) and incubated for at least 30 min at room temperature to achieve alkylation of reduced disulfides. The PDI redox state was then analyzed by standard SDS-PAGE and Western blotting protocols.

Ero1α Redox Isoforms—HeLa cells were transfected with myc-tagged Ero1α expression vector and treated as described for JcM oxidation assay. The ratio of Ero1α redox isoforms (Ox1 and Ox2, Ref. 20) was assessed by standard non-reducing SDS-PAGE and Western blotting protocols.

Glutathione Measurement—Intracellular glutathione was assayed upon formation of S-carboxymethyl derivatives of free thiols with iodoacetic acid, followed by conversion of free amino groups to 2,4-dinitrophenyl derivatives by reaction with 1-fluoro-2,4-dinitrobenzene, as described in Ref. 21. Cells were washed two times with DPBS, scraped in 1 ml of DPBS, centrifuged at low speed, and stored at ±80 °C until GSH measurement by high pressure liquid chromatography, as described previously in Ref. 22. Proteins were determined by the Lowry method (23). Three to eight experiments were performed in triplicate for each sample, and statistical significance was determined by a Student's *t* test.

RESULTS

Soluble Cytosolic Proteins Are Not Essential for Disulfide Bond Formation—To assess the importance of cytosolic factors in controlling disulfide bond formation in the ER, we analyzed oxidative protein folding in semipermeable (SP) cells. Because of the differences in cholesterol content, digitonin permeabilizes the plasma membrane to a much greater extent than the ER or other intracellular organelles (19). Indeed, two cytosolic proteins, endogenous thioredoxin (14.5 kDa) and a transfected red fluorescent protein (26 kDa), disappeared upon digitonin treatment, whereas two ER resident proteins, PDI and ER-yellow fluorescent protein (57 and 27 kDa, respectively), were not affected (Fig. 1). Having validated the system, we analyzed disulfide bond formation using a JcM, as described previously (14). Briefly, intact or SP cells expressing JcM were exposed to DTT to reduce disulfide bonds in ER proteins to synchronize their oxidation. After two washes in cold PBS, cells were incubated for different times in the absence of DTT. Oxidative folding of JcM was monitored by SDS-PAGE in non-reducing conditions. As described previously (14), both intra- and interchain disulfide bonds are formed upon DTT removal, resulting in the accumulation of species migrating with accelerated and retarded mobility, respectively, and in the disappearance of the band corresponding to reduced JcM chains. These processes display similar initial kinetics (14), although, as oxidation proceeds, most oxidized JcM is present as high molecular mass complexes. Moreover, the disappearance of reduced JcM is more representative of JcM oxidation, because isomerization processes might also be involved in the formation of oxidized species (monomers, dimers, and high molecular mass complexes). Therefore, for the sake of brevity, only monomeric JcM are shown in most figures, with one exception (see Fig. 4, in which aggregate formation is investigated).

The kinetics of JcM oxidation were strikingly faster in SP cells than in intact cells (Fig. 2, compare *middle* and *upper panels*, respectively). Re-adding cytosol to SP cells reduced the oxidative folding rate (Fig. 2, *lower panel*), restoring the kinetics observed in intact cells. Because in digitonin-treated cells

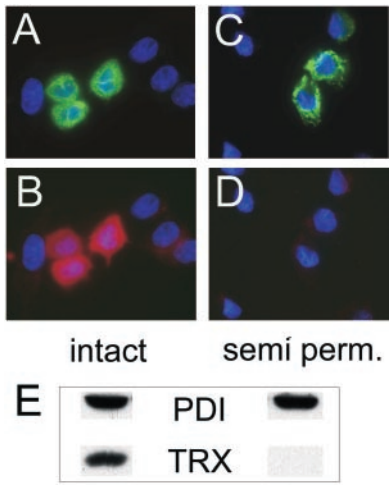

FIG. 1. **Digitonin treatment did not affect ER proteins.** *A–D*, cells transiently transfected with cytosolic red fluorescent protein and ER-localized yellow fluorescent protein were treated with digitonin (*C* and *D*) or were left untreated (*A* and *B*). ER-yellow fluorescent protein was still present after permeabilization (compare *A* with *C*), whereas cytosolic red fluorescent protein was eliminated by digitonin treatment (compare *B* with *D*). *E*, immunoblot of intact and digitonin-treated (*semi perm.*) cell lysates. The cytosolic protein thioredoxin (*TRX*) disappeared after permeabilization, whereas ER resident PDI was unchanged.

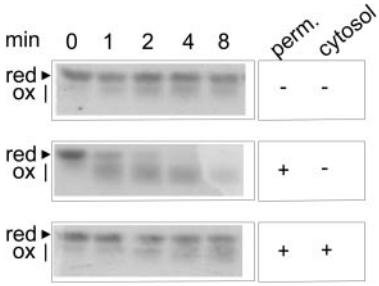

FIG. 2. **Cytosolic factors inhibited JcM oxidation.** Intact or SP HeLa cells expressing JcM were treated with 5 mM DTT to synchronize disulfide bond formation. After elimination of DTT, cells were incubated in DMEM at 24 °C. At the indicated time points, formation of disulfides was blocked by alkylating free thiols with NEM. At 0 min, almost all JcM was in the reduced form (*first lane*, *all panels*). In the absence of cytosol (*middle panel*), JcM oxidation was faster then in intact cells (*upper panel*). Addition of cytosol to SP cells restored the oxidation rate seen in intact cells (*lower panel*).

the oxidation of JcM at 37 °C was almost complete after only 2 min, the experiments were performed at 24 °C to lower the oxidation rate.

The above data demonstrate that soluble cytosolic proteins are dispensable for the formation of disulfide bonds in JcM. On the contrary, the cytosol seems to contain factor(s) which are responsible for the decrease in the oxidation rate of the reporter protein.

GSH Addition Limits JcM Oxidation in SP Cells—In view of the results obtained in yeast (11), we reasoned that the inhibitory effects exerted by the cytosol on disulfide formation could be mediated by reduced glutathione (GSH). The GSH concentration in mammalian cells ranges from 1 to 10 mM (24). Indeed, the addition of 10 mM GSH to SP cells was sufficient to alter the disulfide formation rate to that seen in intact cells. Conversely, 1 mM GSH displayed minor effects (Fig. 3*A*, *third* and *fourth panels*, respectively, and Fig. 3*B*). Adding 10 mM GSH to intact cells had marginal effects upon JcM oxidation (Fig. 3*C*, compare *upper* and *middle left panels*), indicating that either GSH could not cross the plasma membrane or that cytosolic GSH was enough to mask the effect of exogenous molecules.

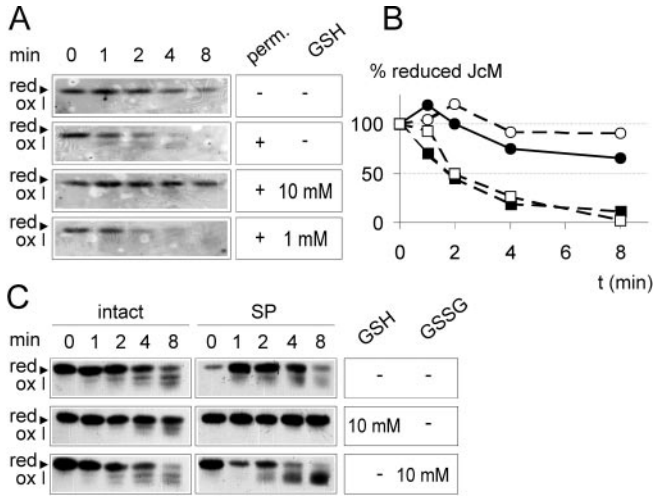

FIG. 3. **GSH limited JcM oxidation in SP cells.** *A*, JcM oxidation was analyzed as described in Fig. 2 in the presence of different concentrations of GSH. The addition of 10 mM GSH (*third panel* down) was sufficient to restore the rate of JcM oxidation to a level comparable with the one seen in intact cells (*upper panel*), as quantified in *B*, where the intensity of the band corresponding to reduced JcM monomers was plotted against time. Data represent the intensity of reduced JcM relative to time 0 in intact cells (●), SP cells (■), SP+10 mM GSH (○), and SP+1 mM GSH (□). *C*, 10 mM GSH or 10 mM GSSG were added to intact or SP cells (*left* and *right panels*, respectively) during JcM oxidation. GSH and GSSG had only minor effects upon JcM oxidation when added to intact cells. At a high concentration (10 mM), oxidized glutathione showed some accelerating effect in SP cells.

The above findings indicate that GSH is effective in limiting JcM oxidation at physiological concentrations and support the idea that glutathione could be the main cytosolic component responsible for buffering disulfide bond formation in the ER. This effect is due to the reducing action of GSH, because the addition of 10 mM GSSG did not inhibit JcM oxidation (Fig. 3*C*).

GSH Depletion in Living Cells Accelerates JcM Oxidation and Induces Aggregate Formation—If GSH were the main factor limiting ER oxidative folding, lowering its pool in intact cells should increase disulfide bond formation. To test this possibility, we treated cells overnight with an inhibitor of glutathione synthesis (BSO), and then with the GSH-inactivating drug DEM (see "Experimental Procedures" for details). Although less markedly than in digitonin-treated cells, the rate of disulfide formation was accelerated in BSO-DEM treated cells (Fig. 4*A*). In contrast, virtually all of the JcM chains remained in the reduced monomer conformation when cells were incubated with DTT (*lanes 16–18*), confirming that degradation was negligible within the time frame of these experiments. Particularly striking was the accumulation of high molecular mass complexes in BSO-DEM-treated cells (*lanes 14–15*). Surprisingly, fewer aggregates were formed in SP cells (*lanes 9-10*), despite the fact that JcM oxidation is faster than in BSO-DEM-treated cells. A possible explanation to this discrepancy was that larger aggregates, either detergent-insoluble or incapable of entering the gels, were formed in SP cells. Therefore, we analyzed the distribution of JcM species in the Nonidet P-40 soluble and insoluble fractions 8 min after DTT removal (Fig. 4*B*). As a further control, an aliquot of cells was incubated with 1 mM diamide, a strong oxidant. In both SP and BSO-DEM-treated cells, abundant high molecular mass covalent complexes containing JcM accumulated at the top of the resolving and in the stacking gel (Fig. 4*B*, *black arrows*). Moreover, JcM aggregates that barely enter the stacking gel and accumulate at the top of the lane (Fig. 4*B*, *white arrow*) are formed in cells that underwent an oxidizing treatment (SP, BSO-DEM, diamide). The Nonidet P-40 insoluble fraction is higher in SP

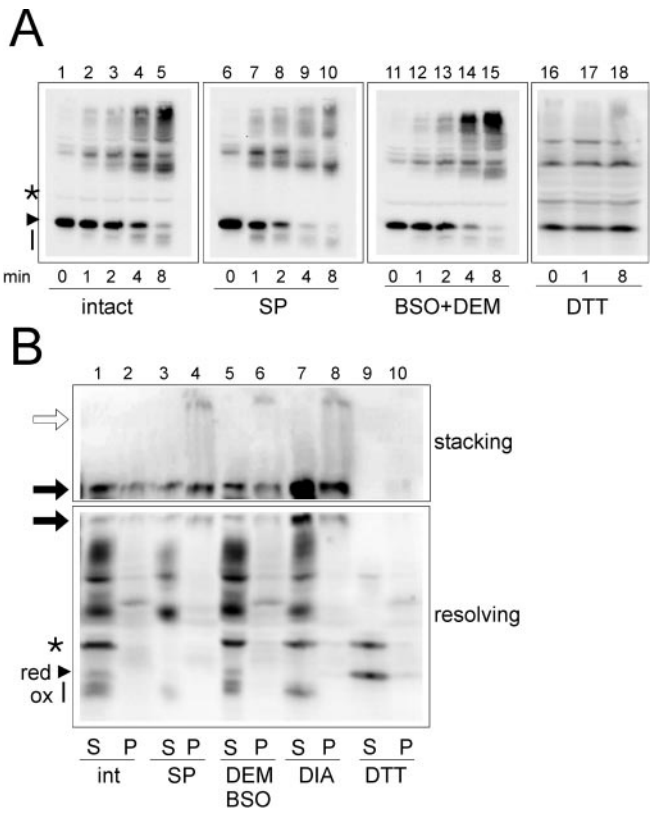

FIG. 4. **GSH depletion in living cells increased JcM oxidation and aggregate formation.** HeLa cells expressing JcM were treated with BSO and DEM (see "Experimental Procedures") to lower the cellular GSH content. *A*, JcM oxidation was analyzed as described in Fig. 2. Intact cells were incubated in medium with (*lanes 16–18*) or without (*lanes 1–5*) 2 mM DTT. Cells previously treated with BSO and DEM (*lanes 11–15*) show an accelerated disulfide formation, resulting in faster disappearance of the reduced monomer and increased formation of high molecular weight complexes. Note that when cells were incubated in DTT, JcM remained largely reduced and was not degraded during the 8 min of incubation (*lanes 16* and *18*). *Arrowheads* and *straight vertical lines*, reduced and oxidized JcM monomers, respectively. *Asterisks*, an unrelated protein disappearing upon digitonin treatment. *B*, the absence of GSH causes the formation of detergent-insoluble high molecular mass JcM aggregates. HeLa cells expressing JcM were treated with 5 mM DTT at 37 °C. After elimination of DTT, cells were incubated 8 min at 24 °C in DMEM containing 1 mM diamide (*DIA*), 2 mM DTT, or nothing. After lysis in Nonidet P-40 buffer, the detergent-soluble and -insoluble fractions were boiled 10 min in Laemmli buffer and analyzed in non-reducing SDS-PAGE. Blots corresponding to stacking and resolving gel are shown, with a higher exposure time for stacking gel (an overlapping area is shown for both exposures). *Black arrows*, high molecular mass complexes at the interface between the resolving and the stacking gel; *white arrows*, complexes barely entering the stacking gel. Although in SP cells less overall material is present, more aggregates accumulated in the insoluble fraction, when compared with BSO/DEM-treated cells. As in many other experiments, the bands corresponding to oxidized monomeric and dimeric JcM chains are more smeared in untreated SP cells than in intact or GSH-supplemented SP cells. This result may reflect decreased isomerization.

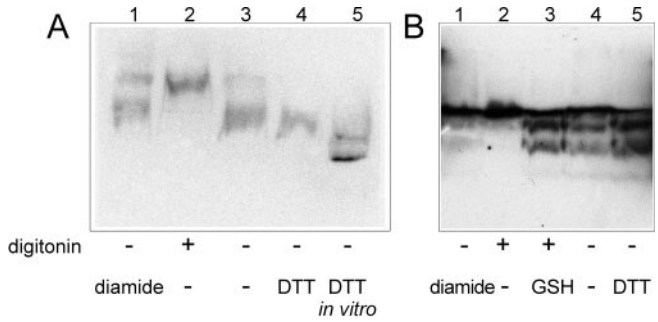

FIG. 5. **Endogenous PDI was more oxidized in SP cells**. *A*, native gels. Total lysates of HeLa cells were resolved by polyacrylamide gels under non-denaturing conditions and immunoblotted against PDI. Diamide and DTT-treated cells were loaded as markers of *in vivo* oxidized and reduced conditions, respectively (*lanes 1* and *4*). *In vitro* reduction was performed by adding 10 mM DTT to the cell lysate (*lane 5*). *Lane 2*, the shift in PDI mobility induced by cytosol elimination. *Lane 3*, endogenous PDI in intact cells. *B*, thiol-accessibility assay. mPEG-maleimide-alkylated samples from HeLa cells treated as indicated (see "Experimental Procedures") were resolved by polyacrylamide SDS-8% PAGE. The more oxidized a protein was at the moment of lysis, the slower was the electrophoretic mobility in this assay. PDI was more oxidized in SP than in intact cells (compare *lanes 2* and *4*), but the change in redox state was reversed by the addition of 10 mM GSH (*lane 3*).

than in BSO-DEM-treated cells. Therefore, the deprivation of either cytosol or GSH accelerates disulfide formation, eventually leading to the formation of high molecular mass, detergent-insoluble, covalent complexes.

The Redox State of PDI Differs in SP Cells—The presence of mixed disulfides between JcM and PDI (14) suggests that formation of disulfide bonds in JcM chains upon DTT removal is catalyzed by PDI. In turn, Ero1α and β are involved in facilitating the oxidation of PDI (14). Therefore, the faster oxidation of JcM chains in SP HeLa cells could be due to an altered redox state of either PDI or Ero1α. To investigate changes in the PDI redox state, we made use of both native gels and alkylation of free thiols with mPEG-maleimide. Electrophoresis in native gels has been shown to discriminate the different redox isoforms of PDI (25), supposedly because of conformational changes. In non-denaturing gels, PDI migrated as a doublet in intact cells (Fig. 5*A*, *lane 3*). Treatment with the reducing agent DTT caused a shift toward the faster species, whereas the reverse was obtained exposing cells to diamide (Fig. 5, *lanes 4* and *1*, respectively). This result suggests that the two bands consisted of different redox isoforms of PDI. Only the slower molecular species was detected in SP cells, suggesting that oxidized PDI is the predominant isoform in SP cells (Fig. 5, *lane 2*). Fig. 5, *lane 5* shows PDI reduced after cell lysis with 10 mM DTT to illustrate the electrophoretic mobility of a PDI molecule that is likely reduced completely.

Similar results are obtained by SDS-PAGE of maleimide-modified samples. As shown in Fig. 5*B*, alkylation of samples with mPEG-maleimide induces changes in PDI electrophoretic mobility according to the redox state of the molecule. A mobility shift consistent with a more oxidized state can be observed in SP cells (*lane 2*), whereas the addition of 10 mM GSH could restore the higher mobility of a more reduced PDI (*lane 3*).

The above findings suggest that cytosolic GSH influences the redox state of PDI, thus modulating its ability to form and isomerize disulfide bonds in cargo proteins.

GSH Modulates the Redox Status of Ero1α—Different Ero1α isoforms are detectable in non-reducing gels, including mixed disulfides with PDI and ERp44 and two distinct bands corresponding to monomeric Ero1α, Ox1 and Ox2 (20, 26). The latter two species are clearly redox-sensitive, as treatment with DTT favors the accumulation of Ox1, whereas the oxidant diamide induces Ox2 (26). Although the functional significance of Ox1 and Ox2 remains to be established, their relative abundance provides an assay to monitor changes in the Ero1α redox state.

Therefore, to determine also whether Ero1α is sensitive to GSH, we monitored the rate of conversion of Ox1 into Ox2 after exposure to DTT in intact and SP cells transfected with myc-tagged Ero1α (Fig. 6). In intact cells, the Ox1/Ox2 ratio is only slightly changed during 8 min at 24 °C of incubation without DTT. In contrast, Ox1 disappears very rapidly in SP cells, and already after 4 min, only the Ox2 form is detectable.

The addition of GSH delays the formation of the Ox2 form in digitonin-treated cells, and this inhibitory effect is dose-dependent (Fig. 6, *third* and *fourth panels*). In fact, inhibition of

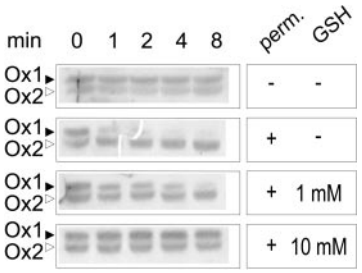

FIG. 6. **GSH affected the redox state of Ero1α.** In HeLa cells transfected with myc-tagged Ero1α, after 5 min of incubation with 5 mM DTT, Ox1 was slightly more abundant than Ox2 in all the conditions tested (*lane 0*, *all panels*). The conversion to the Ox2 form was slower in intact cells than in SP cells, where almost all Ero1α was present as Ox2 after 4 min (*second panel down*, *lane 4*). The addition of GSH decreased the rate of Ox2 formation in a dose-dependent way (*lower panels*).

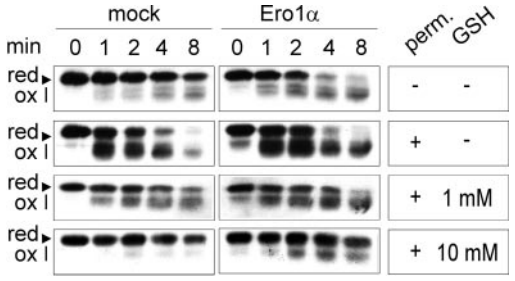

FIG. 7. **Ero1α accelerated JcM oxidation only in the presence of GSH.** HeLa cells expressing JcM were co-transfected with either Ero1α or an empty vector (*mock*). The presence of Ero1α in intact cells accelerated disulfide formation (*first row of panels*), whereas in SP cells, no significant difference could be discerned between mock and Ero1α-transfected cells (*second row of panels*). However, the addition of GSH to SP cells revealed a clear role of Ero1α as a GSH antagonist (*third* and *fourth rows of panels*).

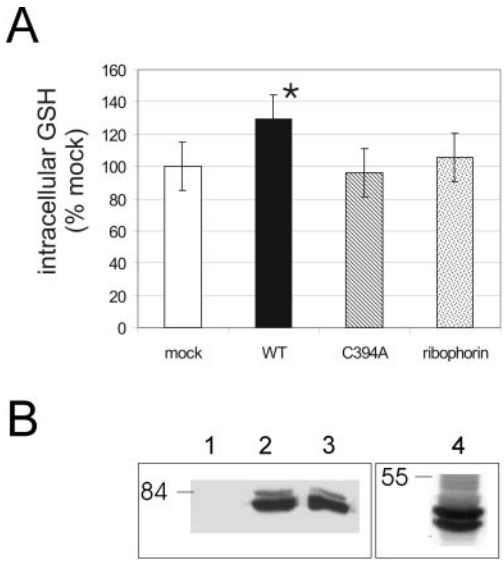

FIG. 8. **Ero1α overexpression increased intracellular GSH.** *A*, the cellular content of GSH was measured by high pressure liquid chromatography in HeLa cells transiently transfected with either empty vector (*white bar*), Ero1α (*black bar*), the Ero1α mutant C394A (*cross hatched bar*), or a mutated ribophorin (*dotted bar*). Only Ero1α gave rise to a significant increase in the intracellular GSH pool. The results are shown as a percentage of mock-transfected cells and represent the average of 3–8 experiments in triplicate. *, $p < 0.01$ (by Student's t test), significant difference from mock. *B*, the levels of transgene expression for a representative experiment. Anti-myc or anti-ribophorin antibodies were used to detect wild-type/mutant Ero1α and ribophorin, respectively. The ribophorin doublet reflects differential utilization of an *N*-glycosylation site. As determined by immunofluorescence, transfection efficiency ranged from 20 to 40%, being generally similar in single experiments, particularly when wild-type and mutant Ero1α vectors were used.

Ox1-Ox2 conversion begins to be detectable at 1 mM GSH, whereas the process was completely restored only at a concentration of GSH (10 mM), which is more similar to that normally present in HeLa cells. These results suggest that GSH can also affect the Ero1α redox state.

Ero1α Antagonizes the Effects of GSH—We have shown in Fig. 5 that PDI is more oxidized in SP cells, suggesting a role for cytosolic GSH in modulating the PDI redox state. On the other hand, it has been demonstrated that Ero1α overexpression is able both to accelerate disulfide formation and to modify the PDI redox state (14). Thus, we wondered whether we could see an effect of Ero1α overexpression also in SP cells. To address this issue, we co-transfected HeLa cells with both Ero1α and JcM and then followed the oxidation of the latter after digitonin treatment in the presence of different GSH concentrations.

Confirming previous data (14), Ero1α overexpression accelerates the rate of JcM oxidation in intact cells (Fig. 7, *upper panels*). Interestingly, however, no significant differences could be seen between Ero1α- and mock-transfected SP cells (Fig. 7, *second row of panels from top*), suggesting that, in the absence of cytosol, a plateau in the oxidation rate was reached. This result is consistent with the fact that PDI is mainly reduced in intact cells, whereas in SP cells, it becomes almost completely oxidized (Fig. 5). However, SP cells overexpressing Ero1α needed more GSH than mock-transfected controls to slow down disulfide formation (Fig. 5, *third* and *bottom lines*). Thus, in cytosol-deprived cells, Ero1α overexpression was ineffective in accelerating JcM oxidation unless GSH was added, further indicating that in intact cells, Ero1α activity may be counterbalanced by cytosolic GSH.

Overexpression of Ero1α Induces the Accumulation of Intracellular GSH—The above results indicate that GSH buffers the oxidative power of Ero1α. This is probably important in living cells, as reduced PDI is needed to isomerize and reduce disulfide bonds during ER quality control (reviewed in Refs. 27 and 28). Indeed, preliminary results from our laboratory indicate that the overexpression of Ero1α inhibits the degradation of several ERAD substrates.[2] In view of the importance of these processes, we decided to determine whether cells are able to respond to excessive ER oxidation by modulating the GSH levels. We found a strong and consistent increase in intracellular GSH in Ero1α-transfected cells, when compared with mock-transfected ones (Fig. 8). The average increase expressed as a percentage of the GSH concentration relative to mock-transfected cells was about 30%. Neither an inactive Ero1α mutant, C394A (12), nor a cysteine-free ribophorin mutant expressed in the ER (29) altered the intracellular GSH levels, confirming the specificity and redox-dependence of the phenomenon. Thus, we conclude that in our cellular system, the overexpression of active Ero1α induces an increase of intracellular GSH.

[2] A. Mezghrani, T. Soldà, C. Fagioli, S. Fabbrini, and R. Sitia, unpublished results.

DISCUSSION

By selectively permeabilizing the plasma membrane, treatment with digitonin allows the removal of soluble cytosolic components and access to the early compartments of the secretory pathway. Because of its low cholesterol contents, the ER membrane maintains its integrity, and the functions of this organelle can be studied independently and easily manipulated in reconstitution assays (Fig. 1, and Ref. 19).

Formation of Disulfide Bonds Does Not Require Soluble Cytosolic Proteins—The fact that disulfide bonds are efficiently formed in SP cells implies that oxidative equivalents can be generated within the ER, where all JcM chains are localized, in the absence of soluble cytosolic proteins. By oxidizing PDI, members of the Ero1 family play a pivotal role in this pathway, which in turn transfers disulfide bonds to nascent proteins via mixed disulfide intermediates (14, 30). In yeast, oxygen accepts electrons from Ero1p in a reaction requiring FAD (31). The observation that human Ero1 molecules complement the Ero1-deficient yeast strain (32) suggests that an analogous mechanism could be active also in mammalian cells.

Cytosolic GSH Limits Disulfide Bond Formation—The faster rate of disulfide formation in SP cells also implies that cytosolic factor(s) limit oxidative folding. Our experiments indicate that this task is largely fulfilled by GSH. Addition of purified GSH slows down disulfide bond formation in a dose-dependent manner; at 10 mM, a GSH concentration within the physiological range for eukaryotic cells (24), JcM oxidation proceeded at the rate observed in intact cells. GSSG was not active, demonstrating the redox dependence of the phenomena. Cysteine accessibility to alkylating agents and native gels were used to monitor the PDI redox state, whereas for Ero1α, we compared the proportions between the redox isoforms Ox1 and Ox2 (20). Although it is not easy to determine precisely the redox state of PDI, our assays reveal significant differences between intact or SP cells, the latter accumulating PDI species that can be increased by diamide in intact cells. With both techniques, we were able to show the co-existence of different redox isoforms at steady state. This might support the idea that PDI, as the key ER oxidoreductase, is concurrently involved in conflicting redox reactions.

It is noteworthy that the rate of Ero1α oxidation following DTT-induced reduction was much faster in the absence of GSH, suggesting that Ero1α is also a target of GSH. Therefore, the two main elements in the process of disulfide bond formation, Ero1α and PDI, are both influenced by cytosolic GSH. Although we cannot exclude the concurrent involvement of other cytosolic reducing systems, namely thioredoxin and NADPH, our results strongly suggest a role for cytosolic GSH in regulating oxidative folding. Lowering the GSH levels in living cells by exposure to BSO and DEM also accelerated JcM oxidation, albeit less than in SP cells. This difference is intriguing, as it may reflect either the existence of additional ways to buffer the ER redox or the utilization of compensatory mechanisms, such as, for instance, the selective delivery of reduced GSH to the ER lumen by enzymatic or transport mechanisms.

Limiting ER Oxidation—The physiological implications of these observations are clear, considering that not only are disulfide bonds formed in the ER, but they must be extensively isomerized during folding (15) and reduced before the dislocation of ER-associated degradation (ERAD) substrates (16). As both reactions are catalyzed by reduced PDI (33, 34), the activity of Ero1α and Ero1β must be limited. Indeed, the overexpression of Ero1α inhibits the degradation of a wide spectrum of ERAD substrates.[2] Our results indicate that cytosolic GSH can reduce PDI, and it cooperates with Ero1α, though working in opposite directions, to establish the proper PDI redox state. In agreement, more GSH is needed to balance oxidative folding in SP cells that overexpress Ero1α, whereas the effects of Ero1α overexpression on the rate of oxidative folding are hardly detectable in the absence of GSH.

In addition to GSH, other factors can generate reduced PDI in living cells. For instance, secretory proteins entering the ER with reduced cysteines likely contribute to consume oxidized PDI, and this may explain why cycloheximide, which blocks protein synthesis, slows down degradation of some ERAD substrates. It is also possible that specific PDI reductases exist, perhaps with a non-uniform distribution within the ER lumen or during development.

Is the ER Environment Really Oxidizing?—The notion that GSH has access to the ER lumen (35, 36) suggests that the ER environment could be much less oxidative than normally assumed. It is not clear how GSH negotiates transport across the ER membrane. Its high concentration in the cytosol provides a strong gradient, but likely specific transporters or channels exist for this charged tripeptide (35, 36). Whatever the mechanism of entry, it is likely that GSH rapidly diffuses within the ER lumen, thus providing a reducing milieu also within this organelle. The function of Ero1 would then be to oxidize PDI by means of specific protein-protein interactions. In principle, this mechanism would generate a default toward reduced PDI. In this redox form, PDI can isomerize and reduce disulfides and, in addition, act as a chaperone endowed with unfoldase activity (33). This may reflect the requirements for stringent quality control systems in higher eukaryotes, where development and intercellular communication depend upon the fidelity of protein secretion.

Regulation of the ER Redox—In most cells, disulfide bond formation depends upon the levels of Ero1α. When these become insufficient to cope with entering polypeptides, the unfolded protein response (UPR)-dependent Ero1β expression could furnish the required oxidative power. In many respects, the periplasmic space of prokaryotes is similar to that of the ER. A fundamental difference, though, is that the oxidation and isomerization/reduction pathways are separated in the periplasmic space, being controlled by the DsbB-DsbA and DsbC-DsbD pathways, respectively. In eukaryotes, instead, PDI is thought to mediate both oxidation and reduction. At first sight, this yin-yang mechanism seems to cause unnecessary complications. However, the redox-dependent conformational changes proposed to regulate unfoldase activity of PDI (37) can offer a unique possibility of coupling precise quality control to the elaboration of disulfide bonds. The import of GSH would set a reducing environment also in the ER, counteracted by a series of protein-protein interactions that allow the targeted delivery of oxidative equivalents. Folding would then make the correct disulfides inaccessible and hence stable. In contrast, misfolded proteins would be easily reduced and, after multiple attempts, targeted for degradation. Insufficient ER redox buffering seems to favor formation of high molecular mass, detergent insoluble, covalent aggregates. These molecular species are likely unproductive and could be dangerous for living cells, causing ER storage diseases (38).

Intercompartment Redox Homeostasis—The cytoplasmic connection via GSH might provide a defense against excessive oxidation produced by the oxidative activity of the ER. The observation that the overexpression of Ero1α induces a significant increase in the reduced glutathione content underscores the relevance of intercompartmental redox control. At present, it is unclear whether the increase in GSH depends upon accelerated synthesis or reduced catabolism-release. Pharmacological induction of a robust UPR with tunicamycin or thapsigargin also increased GSH,[3] confirming the existence of tight links between the ER and the cytosol. The transcription factor ATF4 has recently been shown to couple ER stress to a general cellular response that increases the production of GSH, thus offering protection toward oxidative stress (39). However, the expression of inactive Ero1α mutants or ribophorin 332, a short-lived ER protein devoid of cysteines (29), did not alter the

[3] S. Nerini Molteni, A. Fassio, and R. Sitia, unpublished results.

GSH levels (Fig. 8), thus excluding a major role for cargo-dependent UPR pathways and suggesting that an Ero1-dependent alteration of the ER redox was capable of inducing a cytosolic response. This implies the existence of redox sensors and transducers that transmit information across the ER membrane to modulate GSH metabolism, thus inducing a compensatory response. One attracting possibility is that Ero1α activity generates peroxide (39), thereby eliciting downstream responses to restore the cellular redox homeostasis.

In conclusion, our findings demonstrate that cytosolic GSH counteracts the oxidative power of Ero1α in the ER, likely allowing optimal redox conditions for disulfide isomerization and reduction. The levels of cytoplasmic GSH are influenced by excessive ER oxidation, implying the existence of a tight ER-cytoplasmic connection. Redox-dependent, intercompartmental signaling pathways likely play an important role in cell physiology, allowing the exchange of information across the ER membrane. In this way, cells can rapidly adapt to changing synthetic needs, thus reducing the risks of oxidative stress.

Acknowledgements—We thank all of the members of the laboratory, Adam Benham, Ineke Braakman, Anna Teresa Palamara, and Lars Ellgaard, for helpful criticism, suggestions, and discussions, Tania Mastrandrea for secretarial assistance, and Erwin Ivessa and Adam Benham for providing reagents.

REFERENCES

1. Ellgaard, L., and Helenius, A. (2003) *Nat. Rev. Mol. Cell Biol.* **4,** 181–191
2. Wickner, S., Maurizi, M. R., and Gottesman, S. (1999) *Science* **286,** 1888–1893
3. Fewell, S. W., Travers, K. J., Weissman, J. S., and Brodsky, J. L. (2001) *Annu. Rev. Genet.* **35,** 149–191
4. Blobel, G., and Dobberstein, B. (1975) *J. Cell Biol.* **67,** 835–851
5. Sitia, R., and Braakman, I. (2003) *Nature* **426,** 891–894
6. Fahey, R. C., Hunt, J. S., and Windham, G. C. (1977) *J. Mol. Evol.* **10,** 155–160
7. Thornton, J. M. (1981) *J. Mol. Biol.* **151,** 261–287
8. Knoblach, B., Keller, B. O., Groenendyk, J., Aldred, S., Zheng, J., Lemire, B. D., Li, L., and Michalak, M. (2003) *Mol. Cell. Proteomics* **2,** 1104–1119
9. Hwang, C., Sinskey, A. J., and Lodish, H. F. (1992) *Science* **257,** 1496–1502
10. Frand, A. R., and Kaiser, C. A. (1998) *Mol. Cell* **1,** 161–170
11. Cuozzo, J. W., and Kaiser, C. A. (1999) *Nat. Cell Biol.* **1,** 130–135
12. Cabibbo, A., Pagani, M., Fabbri, M., Rocchi, M., Farmery, M. R., Bulleid, N. J., and Sitia, R. (2000) *J. Biol. Chem.* **275,** 4827–4833
13. Pagani, M., Fabbri, M., Benedetti, C., Fassio, A., Pilati, S., Bulleid, N. J., Cabibbo, A., and Sitia, R. (2000) *J. Biol. Chem.* **275,** 23685–23692
14. Mezghrani, A., Fassio, A., Benham, A., Simmen, T., Braakman, I., and Sitia, R. (2001) *EMBO J.* **20,** 6288–6296
15. Jansens, A., van Duijn, E., and Braakman, I. (2002) *Science* **298,** 2401–2403
16. Fagioli, C., Mezghrani, A., and Sitia, R. (2001) *J. Biol. Chem.* **276,** 40962–40967
17. Yoneda, T., Urano, F., and Ron, D. (2002) *Genes Dev.* **16,** 1307–1313
18. Davis, W., Jr., Ronai, Z., and Tew, K. D. (2001) *J. Pharmacol. Exp. Ther.* **296,** 1–6
19. Wilson, R., Allen, A. J., Oliver, J., Brookman, J. L., High, S., and Bulleid, N. J. (1995) *Biochem. J.* **307,** Pt 3, 679–687
20. Benham, A. M., Cabibbo, A., Fassio, A., Bulleid, N., Sitia, R., and Braakman, I. (2000) *EMBO J.* **19,** 4493–4502
21. Reed, D. J., Babson, J. R., Beatty, P. W., Brodie, A. E., Ellis, W. W., and Potter, D. W. (1980) *Anal. Biochem.* **106,** 55–62
22. Ciriolo, M. R., De Martino, A., Lafavia, E., Rossi, L., Carri, M. T., and Rotilio, G. (2000) *J. Biol. Chem.* **275,** 5065–5072
23. Lowry, O. H., Rosebrough, N. J., Farr, A. L., and Randall, R. J. (1951) *J. Biol. Chem.* **193,** 265–275
24. Meister, A. (1988) *J. Biol. Chem.* **263,** 17205–17208
25. Lumb, R. A., and Bulleid, N. J. (2002) *EMBO J.* **21,** 6763–6770
26. Anelli, T., Alessio, M., Mezghrani, A., Simmen, T., Talamo, F., Bachi, A., and Sitia, R. (2002) *EMBO J.* **21,** 835–844
27. Freedman, R. B., Hirst, T. R., and Tuite, M. F. (1994) *Trends Biochem. Sci.* **19,** 331–336
28. Fassio, A., and Sitia, R. (2002) *Histochem. Cell Biol.* **117,** 151–157
29. de Virgilio, M., Weninger, H., and Ivessa, N. E. (1998) *J. Biol. Chem.* **273,** 9734–9743
30. Frand, A. R., and Kaiser, C. A. (1999) *Mol. Cell* **4,** 469–477
31. Tu, B. P., and Weissman, J. S. (2002) *Mol. Cell* **10,** 983–994
32. Pagani, M., Pilati, S., Bertoli, G., Valsasina, B., and Sitia, R. (2001) *FEBS Lett.* **508,** 117–120
33. Tsai, B., Rodighiero, C., Lencer, W. I., and Rapoport, T. A. (2001) *Cell* **104,** 937–948
34. Molinari, M., Galli, C., Piccaluga, V., Pieren, M., and Paganetti, P. (2002) *J. Cell Biol.* **158,** 247–257
35. Banhegyi, G., Lusini, L., Puskas, F., Rossi, R., Fulceri, R., Braun, L., Mile, V., di Simplicio, P., Mandl, J., and Benedetti, A. (1999) *J. Biol. Chem.* **274,** 12213–12216
36. Feng, W., Liu, G., Allen, P. D., and Pessah, I. N. (2000) *J. Biol. Chem.* **275,** 35902–35907
37. Tsai, B., and Rapoport, T. A. (2002) *J. Cell Biol.* **159,** 207–216
38. Kopito, R. R., and Sitia, R. (2000) *EMBO Rep.* **1,** 225–231
39. Harding, H. P., Zhang, Y., Zeng, H., Novoa, I., Lu, P. D., Calfon, M., Sadri, N., Yun, C., Popko, B., Paules, R., Stojdl, D. F., Bell, J. C., Hettmann, T., Leiden, J. M., and Ron, D. (2003) *Mol. Cell* **11,** 619–633